

## SEQUENTIAL GYROLESS ATTITUDE AND ATTITUDE-RATE ESTIMATION FROM VECTOR OBSERVATIONS†

YAAKOV OSHMAN‡§ and F. LANDIS MARKLEY¶

NASA's Goddard Space Flight Center, Guidance, Navigation and Control Center, Greenbelt, MD, 20771, USA

(Received 8 January 1999)

**Abstract**—A sequential nonlinear estimator is presented for satellite attitude and attitude-rate, which utilizes vector observations in a gyroless setting. The estimator is based on a recently introduced, third-order, minimal-parameter method for solving the attitude matrix kinematic equation. Possessing an extremely simple kinematics, the third-order parameters render the resulting estimator highly computationally efficient. Employing tracking theory concepts, the angular acceleration is modeled as an exponential autocorrelation stochastic process, thus avoiding the use of the uncertain spacecraft dynamic model. An attitude matrix orthogonalization procedure, built into the estimator's scheme, enhances its accuracy and robustness, yet retains reasonable simplicity. The estimator's performance is demonstrated via a Monte Carlo simulation study. © 2000 Elsevier Science Ltd. All rights reserved

## 1. INTRODUCTION

Spacecraft attitude determination from vector observations has been intensively investigated over the last three decades. In most practical implementations of attitude control systems on gyro-based spacecraft, attitude rate information is obtained from an onboard triad of rate gyroscopes. This rate information is used in the propagation stage of an attitude estimator, which utilizes noisy vector observations, resolved in both the body-fixed coordinate system and in a reference system, to estimate the spacecraft attitude and gyro drift rates [1]. Body-fixed vector observations are typically obtained from star trackers, Sun sensors, or magnetometers. Corresponding reference observations, are obtained by using an ephemeris routine (for a Sun observation), or from orbit data and a magnetic field routine (for a magnetic field observation), or from a star catalog (for star observations).

In recent years, with the advent of accurate, high-bandwidth vector sensors (e.g., modern star-trackers), the method of attitude determination from vec-

tor observations has been extended by several researchers to address the estimation of attitude-rate as well, thus facilitating its use on gyroless spacecraft. Gyroless attitude and attitude-rate estimation is, obviously, of prime importance in small, inexpensive spacecraft such as the Solar, Anomalous, Magnetospheric Particle Explorer (SAMPEX), which do not carry gyroscopes but, nevertheless, need to determine their angular velocity for attitude control and attitude propagation purposes. However, even spacecraft which carry gyroscopes can benefit from the use of gyroless attitude-rate estimation during contingency modes.

In Ref. [2], high-bandwidth star-tracker measurements were used to solely drive an error-state extended Kalman filter (EKF), which estimates both the spacecraft attitude quaternion and its angular rate. Challa et al. [3] proposed an attitude and attitude-rate estimator, which utilizes temporal derivatives of vector (Earth's magnetic field) measurements, and dynamically propagates the angular velocity estimates using the nonlinear Euler's equations. A similar concept was employed in Ref. [4], which introduced an angular rate estimator (assuming a known attitude), proposing to alleviate the computational complexity normally associated with the Euler equations-based EKF by using a suboptimal, extended interlaced Kalman filter. In Ref. [5], predictive filtering was applied to estimate the attitude quaternion in a gyroless setting. Using the spacecraft dynamic model, which was assumed to be accurately known, the attitude-rate was estimated as a by-product from the estimated spacecraft angular momentum.

†Paper IAF 97.A2.07 presented at the 48th International Astronautical Congress 6–10 October, 1997, Turin, Italy. This paper is declared a work of the US Government and is not subject to copyright protection in the United States.

‡Associate Professor. This work was performed while the first author spent a sabbatical with NASA's Goddard Space Flight Center as a National Research Council Research Associate. Associate Fellow, AIAA

§Corresponding author: Present address: Technion – Israel Institute of Technology, Department of Aerospace Engineering, Haifa 32000, Israel. e-mail: oshman@technix.technion.ac.il

¶Staff Engineer. Fellow AIAA.

In this paper it is proposed to simultaneously estimate both the attitude matrix and the spacecraft angular velocity from vector measurements. The estimator is based on the recently introduced third-order attitude parametrization method using the integrated-rate parameters (IRP) [6]. Extending the results of Ref. [7], in which vector measurements were used to estimate the attitude in a gyro-based spacecraft, our present work differs from other works addressing the same problem in three main respects. First, the acquired vector measurements are *directly* processed to extract attitude and attitude-rate information, thus avoiding the precomputation of temporal derivatives of these noisy measurements, as required by some other filtering schemes [3,4]. Second, no use is made of the spacecraft dynamic model, which is frequently considered to be highly uncertain, and typically renders the resulting estimator computationally burdensome and sensitive to the uncertainty in the spacecraft inertia tensor. Instead, time propagation of the estimated variables is performed in the proposed filter by modeling the spacecraft angular acceleration as an exponential-autocorrelation stochastic process, and using a polynomial kinematic model, a concept borrowed from tracking theory [8]. Finally, in contrast with other methods relying mainly on the attitude quaternion, the algorithm presented herein directly estimates the attitude matrix, a natural, nonsingular attitude representation. Building upon the minimal IRP third-order parametrization, the new estimator assigns just three state variables for the estimation of the nine-parameter attitude matrix, which is at the heart of its computational efficiency.

In the following section we briefly review the IRP method for the solution of the attitude evolution equation. The angular acceleration kinematic model is presented in Section 3. In Section 4 we develop the filtering stage of the estimator. An attitude matrix orthogonalization procedure, added to enhance the algorithm's accuracy and robustness, is described in Section 5. The prediction stage of the estimator is then derived in Section 6. A numerical study, used to demonstrate the algorithm's performance, is presented in Section 7, followed by concluding remarks in the last section.

## 2. THE IRP METHOD

Consider the matrix differential equation

$$\dot{V}(t) = W(t)V(t), \quad V(t_0) = V_0 \quad (1)$$

where  $V(t) \in \mathbb{R}^{n,n}$ ,  $W(t) = -W^T(t)$  for all  $t \geq t_0$ ,  $V_0 V_0^T = I$  and the raised dot indicates the temporal derivative. This equation arises naturally in three-dimensional (3-D) attitude determination problems, as well as in the square-root solution of the matrix differential Riccati equation [9]. The properties of  $V(t)$  and  $W(t)$  enable a minimal-parameter solution,

which should be much more efficient than a direct solution, based on  $n^2$  straightforward integrations as implied by eqn (1).

First defined by Bar-Itzhack and Markley in Ref. [10], the minimal-parameter problem is to find: (1) a set of  $m = n(n-1)/2$  parameters which unambiguously define  $V(t)$ ; (2) the differential equation satisfied by these parameters; (3) the transformation which maps these parameters into the matrix  $V$ ; and (4) a simple and efficient method to solve the parameters' differential equation and to compute  $V(t)$ .

In Ref. [6], Ronen and Oshman have recently introduced a new, third-order, minimal-parameter method for the solution of eqn (1). The method is based on the skew-symmetric matrix  $A(t, t_0)$ , defined as

$$A(t, t_0) \triangleq \int_{t_0}^t W(\tau) d\tau \quad (2)$$

Using  $A(t, t_0)$ , it can be shown that a third-order approximation of the solution  $V(t)$  is given by

$$\begin{aligned} \tilde{V}(t, t_0) \triangleq & \left\{ I + A(t, t_0) + \frac{A^2(t, t_0)}{2!} + \frac{A^3(t, t_0)}{3!} \right. \\ & \left. + \frac{(t-t_0)}{3!} [A(t, t_0)W_0 - W_0 A(t, t_0)] \right\} V_0 \end{aligned} \quad (3)$$

where  $W_0 = W(t_0)$ . Moreover,  $\tilde{V}$  is a third-order approximation of an orthogonal matrix, in the sense that  $\tilde{V}(t, t_0)\tilde{V}^T(t, t_0) = I + \mathcal{O}((t-t_0)^4)$  where  $\mathcal{O}(x)$  denotes a function of  $x$  that has the property that  $\mathcal{O}(x)/x$  is bounded as  $x \rightarrow 0$ .

Referring to the minimal-parameter problem, the parameters, which define the third-order solution of eqn (1), are the  $n(n-1)/2$  off-diagonal terms of  $A(t, t_0)$ . For the 3-D case, these parameters (termed integrated-rate parameters) have a simple geometric interpretation: they are the angles resulting from a temporal-integration of the three components of the angular velocity vector  $\omega(t) \triangleq [\omega_1(t) \ \omega_2(t) \ \omega_3(t)]^T$ , where  $\omega_i$  is the angular velocity component along the  $i$ -axis of the initial coordinate system, and  $i = 1, 2, 3$  for  $x, y, z$ , respectively. The differential equation satisfied by these parameters is

$$\dot{A}(t, t_0) = W(t), \quad A(t, t_0) = 0 \quad (4)$$

which can be easily solved using any quadrature scheme. Having solved eqn (4), the solution is then used in eqn (3), which yields a third-order, minimal-parameter solution of eqn (1).

In the 3-D case, the orthogonal matrix referred to is the attitude matrix, or the direction cosine matrix (DCM), denoted by  $D(t)$ . The differential equation satisfied by this matrix is the well-known equation

$$\dot{D}(t) = \Omega(t)D(t), \quad D(t_0) = D_0 \quad (5)$$

where  $\Omega(t) = -[\omega(t) \times]$  and  $[\omega(t) \times]$  is the *cross product matrix* corresponding to  $\omega(t)$ , defined as

$$[a \times] \triangleq \begin{bmatrix} 0 & -a_3 & a_2 \\ a_3 & 0 & -a_1 \\ -a_2 & a_1 & 0 \end{bmatrix} \quad \forall a \in \mathbb{R}^3 \quad (6)$$

In this case, the matrix  $A(t, t_0)$  takes the form

$$A(t, t_0) \triangleq -[\theta(t) \times] \quad (7)$$

where the parameter vector  $\theta(t)$  is defined as

$$\theta(t) \triangleq [\theta_1(t) \quad \theta_2(t) \quad \theta_3(t)]^T \quad (8)$$

and

$$\theta_i(t) \triangleq \int_{t_0}^t \omega(\tau) d\tau, \quad i = 1, 2, 3 \quad (9)$$

### 3. STATE SPACE MODEL

Denote the sampling period by  $T \triangleq t_{k+1} - t_k$ . Using the notation  $\theta(k) \triangleq \theta(t_k)$ , the parameter vector at time  $t_k$  is

$$\theta(k) = [\theta_1(k) \quad \theta_2(k) \quad \theta_3(k)]^T \quad (10)$$

and eqn (9) implies

$$\theta_i(k) = \int_{t_0}^{t_k} \omega_i(\tau) d\tau, \quad i = 1, 2, 3 \quad (11)$$

From eqn (11) we have

$$\theta(k+1) = \theta(k) + \int_{t_k}^{t_{k+1}} \omega(\tau) d\tau \quad (12)$$

Defining  $A(k+1, k)$  to be the discrete-time analog of  $A(t, t_0)$ , i.e.,

$$A(k+1, k) \triangleq -[(\theta(k+1) - \theta(k)) \times] \quad (13)$$

eqn (3) is rewritten as

$$\begin{aligned} D(k+1) = & \left\{ I + A(k+1, k) + \frac{1}{2} A^2(k+1, \right. \\ & k) + \frac{1}{6} A^3(k+1, k) + \frac{1}{6} T[A(k+1, \\ & k)\Omega(k) - \Omega(k)A(k+1, k)] \left. \right\} D(k) \end{aligned} \quad (14)$$

To avoid using the uncertain spacecraft dynamic model, the spacecraft angular acceleration is modeled as a zero-mean stochastic process with exponential autocorrelation function. The acceleration dynamic model is, therefore, the following first-order Markov process,

$$\dot{\omega}(t) = -\Psi\dot{\omega}(t) + \tilde{v}(t) \quad (15)$$

For simplicity, a decoupled kinematic model is chosen for the three angular rate components, i.e.,

$$\Psi \triangleq \text{diag} \left\{ \frac{1}{\tau_1}, \frac{1}{\tau_2}, \frac{1}{\tau_3} \right\} \quad (16)$$

where  $\{\tau_i\}_{i=1}^3$  are the acceleration decorrelation times along the corresponding body axes. The driv-

ing noise is a zero-mean white process, with

$$E\tilde{v}(t)\tilde{v}(s) = \tilde{Q}(t)\delta(t-s) \quad (17)$$

and the power spectral density (PSD) matrix is

$$\tilde{Q}(t) = 2\Psi\Sigma^2 \quad (18)$$

where

$$\Sigma \triangleq \text{diag}\{\sigma_1, \sigma_2, \sigma_3\} \quad (19)$$

To determine the noise variances in eqn (19), the following angular acceleration probabilistic model is used [8]: the angular acceleration components,  $\{\dot{\omega}_i\}_{i=1}^3$ , can be (1) equal to  $\dot{\omega}_{M_i}$  with probability  $p_{M_i}$ ; (2) equal to  $-\dot{\omega}_{M_i}$  with probability  $p_{M_i}$ ; (3) equal to zero with probability  $p_0$ ; or (4) uniformly distributed over the interval  $[-\dot{\omega}_{M_i}, \dot{\omega}_{M_i}]$  with the remaining probability mass. Using this model, it follows that

$$\sigma_i^2 = \frac{\dot{\omega}_{M_i}^2}{3}(1 + 4p_{M_i} - p_0) \quad (20)$$

Now let the system's state vector be defined as

$$x(t) \triangleq [\theta^T(t) \quad \omega^T(t) \quad \dot{\omega}^T(t)]^T \quad (21)$$

then the state equation is

$$\dot{x}(t) = Fx(t) + \tilde{v}(t) \equiv \begin{bmatrix} 0 & I & 0 \\ 0 & 0 & I \\ 0 & 0 & -\Psi \end{bmatrix} x(t) + \begin{bmatrix} 0 \\ 0 \\ \tilde{v}(t) \end{bmatrix}$$

with obvious definitions of  $F$  and  $\tilde{v}(t)$ . Corresponding to the sampling interval  $T$ , the discrete-time state equation is

$$x(k+1) = e^{FT}x(k) + \tilde{v}(k) \quad (22)$$

where the transition matrix is expressed by

$$e^{FT} = \begin{bmatrix} I & TI & \Psi^{-2}(e^{-\Psi T} - I + T\Psi) \\ 0 & I & \Psi^{-1}(I - e^{-\Psi T}) \\ 0 & 0 & e^{-\Psi T} \end{bmatrix} \quad (23)$$

and  $v(k)$  is a zero-mean, white noise sequence, with covariance

$$\begin{aligned} Q(k) \triangleq E v(k)v^T(k) = & \int_0^T e^{F(T-t)} \text{diag}\{0, 0, \\ & \tilde{Q}(t)\} e^{F^T(T-t)} dt \end{aligned} \quad (24)$$

#### 3.1. Filter model

Since, upon observing eqn (14), the attitude matrix at time  $t_{k+1}$  is expressed in terms of the IRP vector at  $t_{k+1}$  and the angular rate at  $t_k$ , it will be useful for the development in the sequel to define the *filter* state vector as

$$x_f(k+1) \triangleq [\theta^T(k+1)\omega^T(k)\dot{\omega}^T(k)]^T \quad (25)$$

It is easy to see that the state equation for the filter state vector is

$$x_f(k+1) = \Phi(T)x_f(k) + \Gamma(T)v_f(k)$$

$$\tilde{x}_f(j|k) \triangleq x_f(j) - \hat{x}_f(j|k) \quad (28)$$

$$\begin{aligned} & \equiv \begin{bmatrix} I & TI & T\Phi_{23}(T) + \Phi_{13}(T)\Phi_{33}(T) \\ 0 & I & \Phi_{23}(T) \\ 0 & 0 & \Phi_{33}(T) \end{bmatrix} x_f(k) \\ & + \begin{bmatrix} I & TI & \Phi_{13}(T) \\ 0 & I & 0 \\ 0 & 0 & I \end{bmatrix} v_f(k) \end{aligned} \quad (26)$$

where the effective process noise  $v_f$  is a zero-mean sequence with

$$Q_f(k) \triangleq E v_f(k) v_f^T(k) = \begin{bmatrix} Q_{11}(k) & 0 & 0 \\ 0 & Q_{22}(k) & Q_{23}(k) \\ 0 & Q_{32}(k) & Q_{33}(k) \end{bmatrix}$$

and the block matrices appearing in eqn (26) are

$$\Phi_{13}(T) \triangleq \Psi^{-2}(e^{-\Psi T} - I + \Psi T) \quad (27a)$$

$$\Phi_{23}(T) \triangleq \Psi^{-1}(I - e^{-\Psi T}) \quad (27b)$$

$$\Phi_{33}(T) \triangleq e^{-\Psi T} \quad (27c)$$

The non-zero entries of  $Q_f(k)$  are obtained by explicitly computing the integrals in eqn (24), which yields

$$Q_{11}(k) = \Psi^{-4} \Sigma^2 \left( I + 2\Psi T - 2\Psi^2 T^2 + \frac{2}{3} \Psi^3 T^3 - e^{-2\Psi T} - 4\Psi T e^{-\Psi T} \right)$$

$$Q_{22}(k) = \Psi^{-2} \Sigma^2 (4e^{-\Psi T} - 3I - e^{-2\Psi T} + 2\Psi T)$$

$$Q_{23}(k) = Q_{32}(k) = \Psi^{-1} \Sigma^2 (e^{-2\Psi T} + I - 2e^{-\Psi T})$$

$$Q_{33}(k) = \Sigma^2 (I - e^{-2\Psi T})$$

In passing, it is noted that the effective process noise  $v_f$  is a time-correlated sequence. In principle, standard methods, dealing with the case of colored process noise, could be employed. However, since this correlation is weak, and in view of the fact that practically every state estimator requires a tuning process, in which the process noise covariance matrix is empirically adjusted, this correlation will be neglected in the sequel.

#### 4. VECTOR MEASUREMENT PROCESSING

Let the minimum mean-squared error (MMSE) estimates of  $\theta(k+1)$  and  $\omega(k)$ , based on measurements up to and including  $t_k$ , be denoted by  $\hat{\theta}(k+1|k)$  and  $\hat{\omega}(k|k)$ , respectively. Assume that at  $t_{k+1}$  we have on hand the predicted vector  $\hat{x}_f(k+1|k)$  and its corresponding prediction error covariance matrix,  $P(k+1|k) \triangleq E\{\tilde{x}_f(k+1|k)\tilde{x}_f^T(k+1|k)\}$ , where the estimation error is defined as

As the first step in developing the measurement update algorithm, we next formulate the observation equation.

##### 4.1. Observation equation

Let  $\mathcal{S}_u$  and  $\mathcal{S}_v$  denote the reference Cartesian coordinate system and the body-fixed Cartesian coordinate system, respectively. The new pair of corresponding noisy vector measurements at  $t_{k+1}$  consists of the *unit* vectors  $u(k+1)$  and  $v(k+1)$ , which represent the *measured* values of the same vector  $r(k+1)$ , resolved in  $\mathcal{S}_u$  and in  $\mathcal{S}_v$ , respectively. The direction-cosine matrix  $D(k+1)$ , representing the true attitude of  $\mathcal{S}_v$  relative to  $\mathcal{S}_u$  at time  $t_{k+1}$ , transforms the *true* vector representation  $u_0$  in  $\mathcal{S}_u$  into its corresponding *true* representation  $v_0$  in  $\mathcal{S}_v$  according to

$$v_0(k+1) = D(k+1)u_0(k+1) \quad (29)$$

The measured vectors are assumed to be related to the true vectors according to

$$v(k+1) = v_0(k+1) + n_v(k+1) \quad (30)$$

$$u(k+1) = u_0(k+1) + n_u(k+1) \quad (31)$$

where the measurement noises are white, Gaussian, mutually uncorrelated sequences, with

$$n_v(k+1) \sim \mathcal{N}(0, R_v(k+1)) \quad (32)$$

$$n_u(k+1) \sim \mathcal{N}(0, R_u(k+1)) \quad (33)$$

and  $R_u(k)$  and  $R_v(k)$  are known covariance matrices.

To relate the information contained in the measurements to the state vector at  $t_{k+1}$ , eqn (29) is rewritten as

$$v_0(k+1) = D[\theta(k+1) - \theta(k), \omega(k), D(k)] u_0(k+1) \quad (34)$$

where the notation  $D[\theta(k+1) - \theta(k), \omega(k), D(k)]$  reflects the fact that, by eqn (13) and (14), the attitude at time  $t_{k+1}$  is related to the attitude at time  $t_k$  via the IRP vector difference  $\theta(k+1) - \theta(k)$  and the angular rate vector  $\omega(k)$ .

To process the information contained in the new vector measurements, the nonlinear measurement eqn (34) is next linearized about a *nominal* state, consisting of the most recent estimates. Assuming that after the previous measurement update (at  $t_k$ ) linearization has been performed about the *a posteriori* state estimate, the resulting *nominal* state vector at  $t_{k+1}$  is the predicted estimate,  $\hat{x}_f(k+1|k)$ . Therefore, the predicted state vector is assumed to be related to the true one according to

$$x_f(k+1) = \hat{x}_f(k+1|k) + \delta x_f(k+1)$$

$$\equiv \begin{bmatrix} \hat{\theta}(k+1|k) \\ \hat{\omega}(k|k) \\ \hat{\dot{\omega}}(k|k) \end{bmatrix} + \begin{bmatrix} \delta\theta(k+1) \\ \delta\omega(k+1) \\ \delta\dot{\omega}(k+1) \end{bmatrix} \quad (35)$$

where  $\delta\theta(k+1)$ ,  $\delta\omega(k+1)$  and  $\delta\dot{\omega}(k+1)$  are the perturbations of the state components about the nominal (i.e., predicted) state. Let  $\hat{D}^*(k|k)$  denote the *a posteriori*, *orthogonalized* estimate of the attitude matrix at time  $t_k$ , to be discussed in the next section. Using now the most recent estimates for  $D(k)$  and  $x_f(k)$ , namely  $\hat{D}^*(k|k)$  and  $\hat{x}_f(k|k)$ , respectively, in eqn (34), it follows from eqns (30), (31) and (35) that

$$v(k+1) - n_v(k+1) = D \left[ \hat{\theta}(k+1|k) \right. \\ \left. + \delta\theta(k+1) - \hat{\theta}(k|k), \hat{\omega}(k|k) \right. \\ \left. + \delta\omega(k+1), \hat{D}^*(k|k) \right] \times [u(k+1) \\ - n_u(k+1)] \quad (36)$$

As discussed in the sequel, the *a posteriori* IRP estimate is zeroed after each measurement update (due to full reset control of the IRP state). We will, therefore, use the reset value of the IRP estimate,  $\theta^c(k|k) = 0$ , in eqn (36). Now expand  $D$  about the nominal state using a first-order Taylor series expansion, i.e.,

$$D \left[ \hat{\theta}(k+1|k) + \delta\theta(k+1), \hat{\omega}(k|k) + \delta\omega(k+1), \right. \\ \left. \hat{D}^*(k|k) \right] = \hat{D}(k+1|k) \\ + \sum_{i=1}^3 \frac{\partial D \left[ \theta(k+1), \hat{\omega}(k|k), \hat{D}^*(k|k) \right]}{\partial \theta_i} \Bigg|_{\hat{\theta}(k+1|k)} \\ \times \delta\theta_i(k+1) \\ + \sum_{i=1}^3 \frac{\partial D \left[ \hat{\theta}(k+1|k), \omega(k), \hat{D}^*(k|k) \right]}{\partial \omega_i} \Bigg|_{\hat{\omega}(k|k)} \\ \times \delta\omega_i(k+1) \quad (37)$$

where  $()|_{\zeta}$  denotes ‘evaluated at  $\zeta$ ’ and

$$\hat{D}(k+1|k) \triangleq D \left[ \hat{\theta}(k+1|k), \hat{\omega}(k|k), \hat{D}^*(k|k) \right]$$

(see Section 6). Using eqn (14), the sensitivity matrices appearing in eqn (37) are expressed as

$$\frac{\partial}{\partial \theta_i} D \left[ \theta(k+1), \hat{\omega}(k|k), \right. \\ \left. \hat{D}^*(k|k) \right] = G_i \left[ \theta(k+1), \hat{\omega}(k|k) \right] \hat{D}^*(k|k) \quad (38a)$$

$$\frac{\partial}{\partial \omega_i} D \left[ \hat{\theta}(k+1|k), \omega(k), \right. \\ \left. \hat{D}^*(k|k) \right] = F_i \left[ \hat{\theta}(k+1|k) \right] \hat{D}^*(k|k) \quad (38b)$$

for  $i = 1, 2, 3$ , where the sensitivity matrices

Table 1. Sensitivity matrices

$$G_1(\theta, \omega) = \begin{bmatrix} 0 & \frac{1}{2}\theta_2 - \frac{1}{3}\theta_1\theta_3 - \frac{1}{6}T\omega_2 & \frac{1}{2}\theta_3 + \frac{1}{3}\theta_1\theta_2 - \frac{1}{6}T\omega_3 \\ \frac{1}{2}\theta_2 + \frac{1}{3}\theta_1\theta_3 + \frac{1}{6}T\omega_2 & -\theta_1 & 1 - \frac{1}{6}(\theta_2^2 + \theta_3^2) - \frac{1}{2}\theta_1^2 \\ \frac{1}{2}\theta_3 - \frac{1}{3}\theta_1\theta_2 + \frac{1}{6}T\omega_3 & -1 + \frac{1}{6}(\theta_2^2 + \theta_3^2) + \frac{1}{2}\theta_1^2 & -\theta_1 \end{bmatrix}$$

$$G_2(\theta, \omega) = \begin{bmatrix} -\theta_2 & \frac{1}{2}\theta_1 - \frac{1}{3}\theta_2\theta_3 + \frac{1}{6}T\omega_1 & -1 + \frac{1}{6}(\theta_1^2 + \theta_3^2) + \frac{1}{2}\theta_2^2 \\ \frac{1}{2}\theta_1 + \frac{1}{3}\theta_2\theta_3 - \frac{1}{6}T\omega_1 & 0 & \frac{1}{2}\theta_3 - \frac{1}{3}\theta_1\theta_2 - \frac{1}{6}T\omega_3 \\ 1 - \frac{1}{6}(\theta_1^2 + \theta_3^2) - \frac{1}{2}\theta_2^2 & \frac{1}{2}\theta_3 + \frac{1}{3}\theta_1\theta_2 + \frac{1}{6}T\omega_3 & -\theta_2 \end{bmatrix}$$

$$G_3(\theta, \omega) = \begin{bmatrix} -\theta_3 & 1 - \frac{1}{6}(\theta_1^2 + \theta_2^2) - \frac{1}{2}\theta_3^2 & \frac{1}{2}\theta_1 + \frac{1}{3}\theta_2\theta_3 + \frac{1}{6}T\omega_1 \\ -1 + \frac{1}{6}(\theta_1^2 + \theta_2^2) + \frac{1}{2}\theta_3^2 & -\theta_3 & \frac{1}{2}\theta_2 - \frac{1}{3}\theta_1\theta_3 + \frac{1}{6}T\omega_2 \\ \frac{1}{2}\theta_1 - \frac{1}{3}\theta_2\theta_3 - \frac{1}{6}T\omega_1 & \frac{1}{2}\theta_2 + \frac{1}{3}\theta_1\theta_3 - \frac{1}{6}T\omega_2 & 0 \end{bmatrix}$$

$$F_1(\theta) = \frac{1}{6}T \begin{bmatrix} 0 & \theta_2 & \theta_3 \\ -\theta_2 & 0 & 0 \\ -\theta_3 & 0 & 0 \end{bmatrix} \quad F_2(\theta) = \frac{1}{6}T \begin{bmatrix} 0 & -\theta_1 & 0 \\ \theta_1 & 0 & \theta_3 \\ 0 & -\theta_3 & 0 \end{bmatrix} \quad F_3(\theta) = \frac{1}{6}T \begin{bmatrix} 0 & 0 & -\theta_1 \\ 0 & 0 & -\theta_2 \\ \theta_1 & \theta_2 & 0 \end{bmatrix}$$

$\{G_i, F_i\}_{i=1}^3$  are shown in Table 1. Using eqn (37) in eqn (36) and neglecting second-order terms yields

$$\begin{aligned} & \nu(k+1) - \hat{D}(k+1|k)u(k+1) \\ &= \sum_{i=1}^3 \left[ G_i \left[ \hat{\theta}(k+1|k), \hat{\omega}(k|k) \right] \hat{D}^*(k|k) \delta\theta_i(k+1) \right. \\ & \quad \left. + F_i \left[ \hat{\theta}(k+1|k) \right] \hat{D}^*(k|k) \delta\omega_i(k+1) \right] u(k+1) \\ & \quad - \hat{D}(k+1|k)n_u(k+1) + n_v(k+1) \\ &= H(k+1) \begin{bmatrix} \delta\theta(k+1) \\ \delta\omega(k+1) \\ \delta\dot{\omega}(k+1) \end{bmatrix} \\ & \quad - \hat{D}(k+1|k)n_u(k+1) + n_v(k+1) \end{aligned} \quad (39)$$

where the observation matrix  $H(k+1)$  is written in block matrix form as

$$H(k+1) \equiv \begin{bmatrix} H_1(k+1) & H_2(k+1) & 0 \end{bmatrix} \in \mathbb{R}^{3,9}$$

and the columns of the submatrices  $H_1(k+1) \in \mathbb{R}^{3,3}$  and  $H_2(k+1) \in \mathbb{R}^{3,3}$  are

$$\begin{aligned} H_{1i}(k+1) &= G_i \left[ \hat{\theta}(k+1|k), \right. \\ & \quad \left. \hat{\omega}(k|k) \right] \hat{D}^*(k|k) u(k+1) \end{aligned}$$

$$H_{2i}(k+1) = F_i \left[ \hat{\theta}(k+1|k) \right] \hat{D}^*(k|k) u(k+1)$$

for  $i = 1, 2, 3$ . Define now the *effective* measurement and measurement noise to be, respectively,

$$y(k+1) \triangleq \nu(k+1) - \hat{D}(k+1|k)u(k+1) \quad (41)$$

$$n(k+1) \triangleq n_v(k+1) - \hat{D}(k+1|k)n_u(k+1) \quad (42)$$

Then, using these definitions in eqn (39) yields the following measurement, equation:

$$y(k+1) = H(k+1)\delta x_f(k+1) + n(k+1) \quad (43)$$

The measurement noise is a white, Gaussian sequence with

$$n(k+1) \sim \mathcal{N}(0, R(k+1)) \quad (44)$$

where

$$\begin{aligned} R(k+1) &\triangleq R_v(k+1) \\ & \quad + \hat{D}(k+1|k)R_u(k+1)\hat{D}^T(k+1|k) \end{aligned} \quad (45)$$

#### 4.2. Measurement update

From eqns (28) and (35) it follows that

$$\begin{aligned} \delta x_f(k+1) &= x_f(k+1) - \hat{x}_f(k+1|k) \\ &= \tilde{x}_f(k+1|k) \end{aligned} \quad (46)$$

Since  $\hat{x}_f(k+1|k)$  is an unbiased, MMSE predictor, we have

$$E\{\delta x_f(k+1)\} = E\{\tilde{x}_f(k+1|k)\} = 0$$

and

$$\text{cov}\{\delta x_f(k+1)\} = \text{cov}\{\tilde{x}_f(k+1|k)\} = P(k+1|k)$$

yielding

$$\delta x_f(k+1) \sim \mathcal{N}(0, P(k+1|k)) \quad (47)$$

Using the linearized measurement eqn (43) and the statistical properties of the measurement and prediction errors, eqns (44) and (47), respectively, the MMSE estimator of  $\delta x_f(k+1)$  is [11]

$$\widehat{\delta x}_f(k+1|k+1) = K(k+1)y(k+1) \quad (48)$$

where  $K(k+1)$ , the estimator gain matrix, is computed as

$$\begin{aligned} K(k+1) &= P(k+1|k)H^T(k+1) \\ & \quad \times [H(k+1)P(k+1|k)H^T(k+1) + R(k+1)]^{-1} \end{aligned}$$

Also, from eqn (46) we have

$$\widehat{\delta x}_f(k+1|k+1) = \hat{x}_f(k+1|k+1) - \hat{x}_f(k+1|k)$$

which, used in eqn (48), yields the state measurement update equation

$$\hat{x}_f(k+1|k+1) = \hat{x}_f(k+1|k) + K(k+1)y(k+1)$$

To derive the covariance update equation, we subtract  $x_f(k+1)$  from both sides of the last equation and use eqns (43) and (46) to obtain

$$\begin{aligned} \hat{x}_f(k+1|k+1) &= [I - K(k+1) \\ & \quad \times H(k+1)]\hat{x}_f(k+1|k) - K(k+1)n(k+1) \end{aligned} \quad (49)$$

from which the resulting covariance update equation is

$$\begin{aligned} P(k+1|k+1) &= [I - K(k+1)H(k+1)] \\ & \quad \times P(k+1|k)[I - K(k+1)H(k+1)]^T \\ & \quad + K(k+1)R(k+1)K^T(k+1) \end{aligned} \quad (50)$$

where the filtering error covariance matrix  $P(k+1|k+1)$  is defined analogously to  $P(k+1|k)$ .

To compute the measurement-update attitude matrix at time  $t_{k+1}$ , we use the most recent estimate  $\hat{x}_f(k+1|k+1)$  and the estimated attitude matrix corresponding to time  $t_k$  in eqn (14). This yields

$$\hat{D}(k+1|k+1) = \left\{ I + \hat{A}(k+1, k) + \frac{1}{2} \hat{A}^2(k+1, k) + \frac{1}{6} \hat{A}^3(k+1, k) + \frac{1}{6} T \left[ \hat{A}(k+1, k) \hat{\Omega}(k|k+1) - \hat{\Omega}(k|k+1) \hat{A}(k+1, k) \right] \right\} \hat{D}^*(k|k) \quad (51)$$

where the *a posteriori* estimates of  $A(k+1, k)$  and  $\Omega(k)$  are defined, respectively, as

$$\hat{A}(k+1, k) \triangleq - \left[ \hat{\theta}(k+1|k+1) \times \right] \quad (52)$$

$$\hat{\Omega}(k|k+1) \triangleq - \left[ \hat{\omega}(k|k+1) \times \right] \quad (53)$$

Finally, since the *a posteriori* attitude matrix  $\hat{D}(k+1|k+1)$ , is computed based on the *a posteriori* estimate,  $\theta(k+1|k+1)$ , this implies a full *reset*

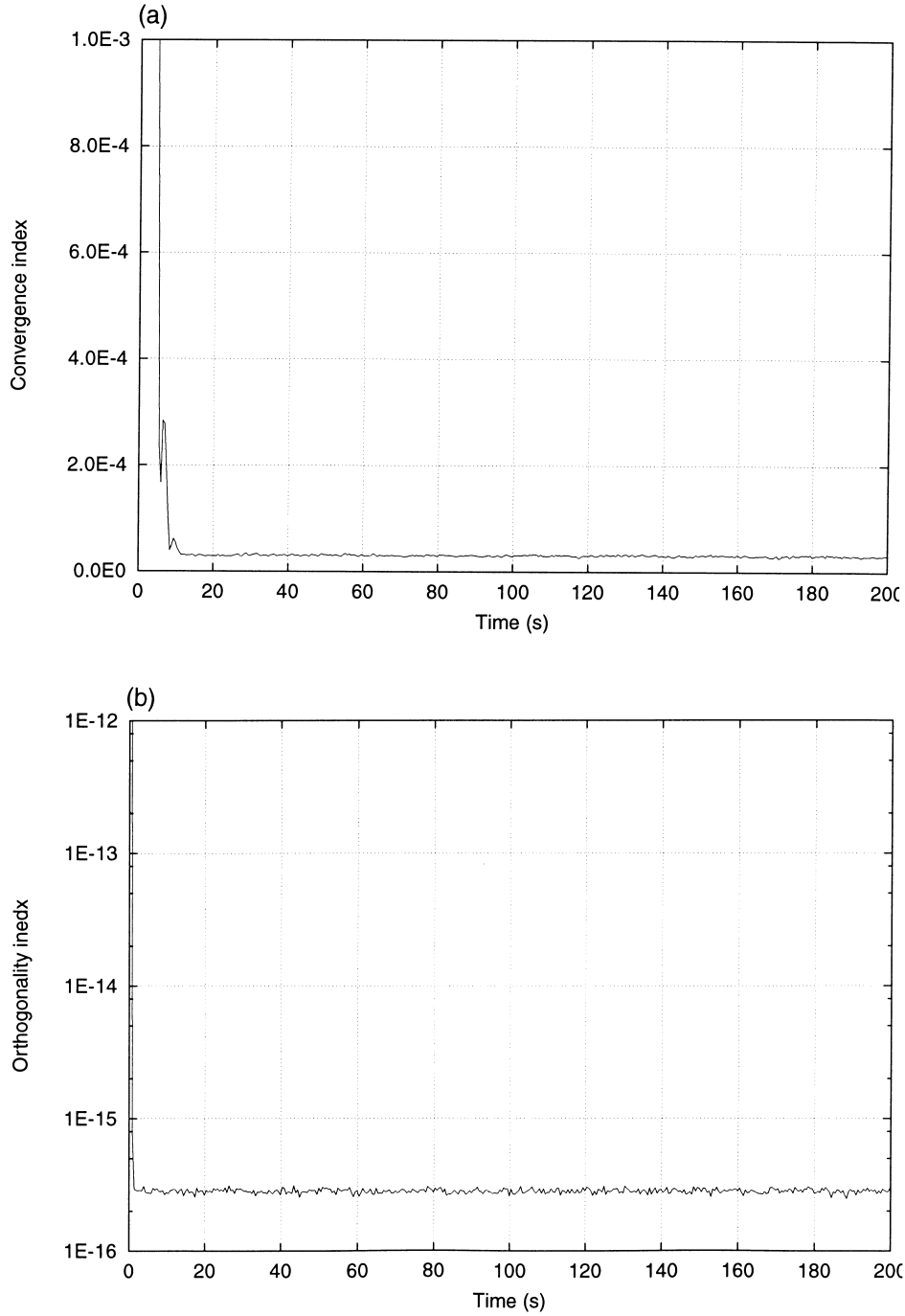


Fig. 1. Performance indices based on a Monte Carlo simulation study (100 runs): (a) convergence index; (b) orthogonality index.

control of the parameter vector, i.e.,

$$\theta^c(k+1) = \theta(k+1) - \hat{\theta}(k+1 | k+1) \quad (54)$$

where  $\theta^c(k+1)$  is the *reset* state vector at  $t_{k+1}$ , and a corresponding reset of the state estimate

$$\hat{\theta}^c(k+1 | k+1) = 0 \quad (55)$$

5. ATTITUDE MATRIX ORTHOGONALIZATION

Due to numerical implementation errors, linearization approximations and the third-order nature of the attitude parametrizations used, the estimated attitude matrix will not be orthogonal. To improve

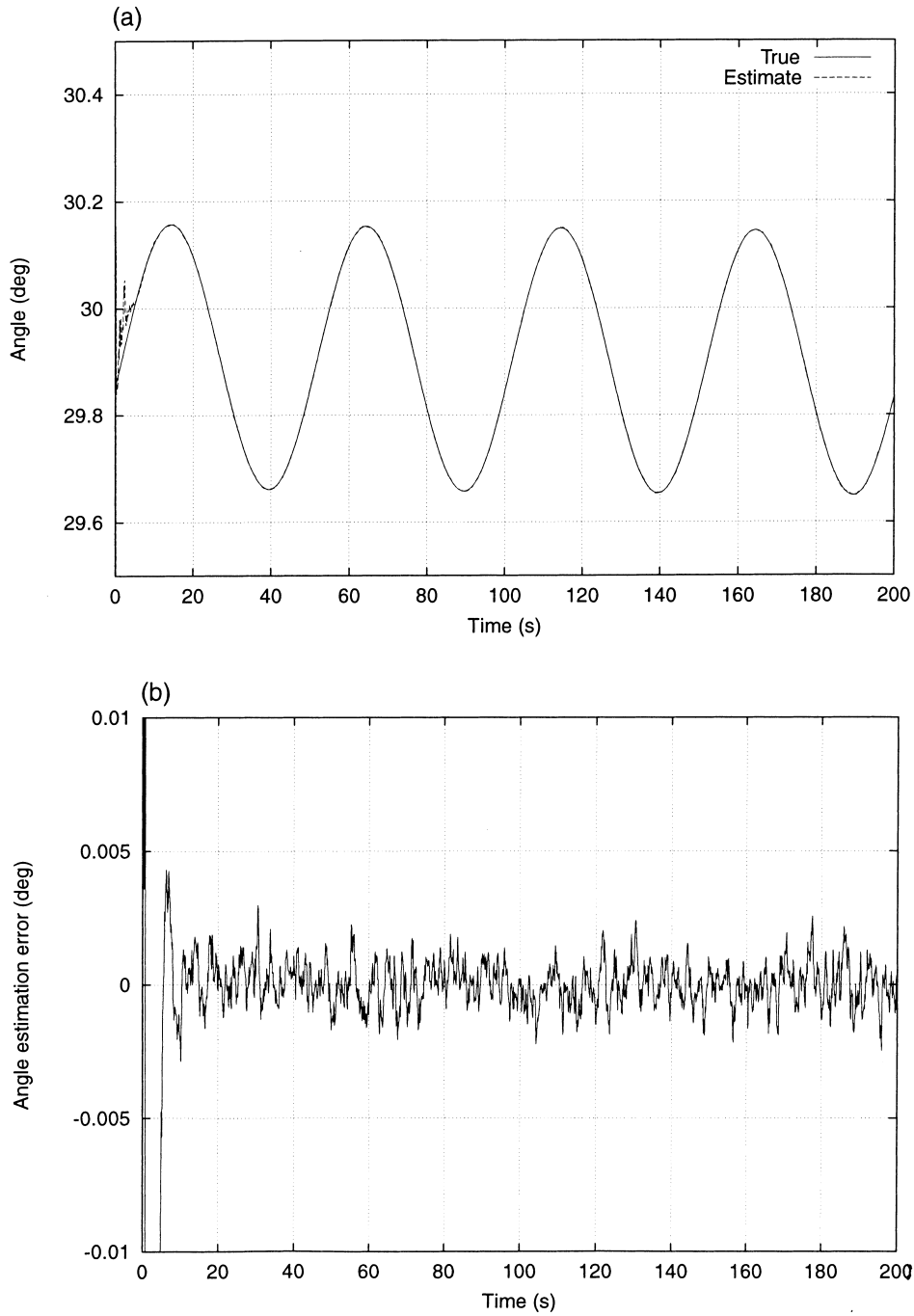


Fig. 2. Estimated vs. true Euler angles in a typical simulation run (a) Roll angle. (b) Roll angle estimation error. (c) Pitch angle. (d) Pitch angle estimation error. (e) Yaw angle. (f) Yaw angle estimation error.



the algorithm's accuracy and enhance its stability, an additional orthogonalization procedure is introduced into the estimator, following the measurement update stage. In this procedure, the orthogonal matrix closest to the filtered attitude matrix is computed.

Given the filtered attitude matrix  $\hat{D}(k + 1|k + 1)$ , the matrix orthogonalization problem is to find the

matrix

$$\hat{D}^*(k + 1 | k + 1) \triangleq \arg \min_{D \in \mathbb{R}^{3,3}} \| \hat{D}(k + 1 | k + 1) - D \|$$

subject to

$$D^T D = I$$

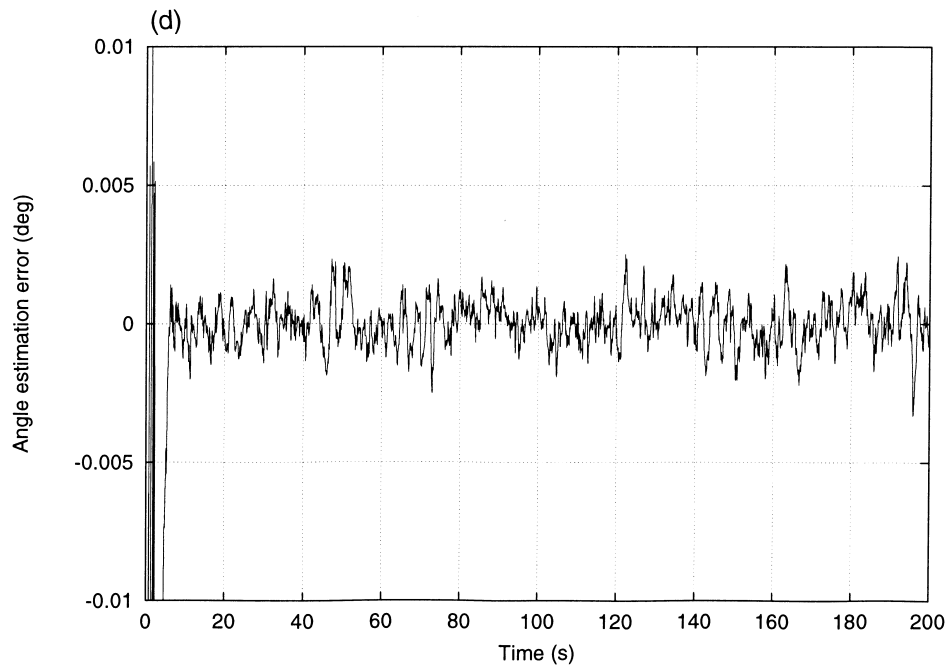
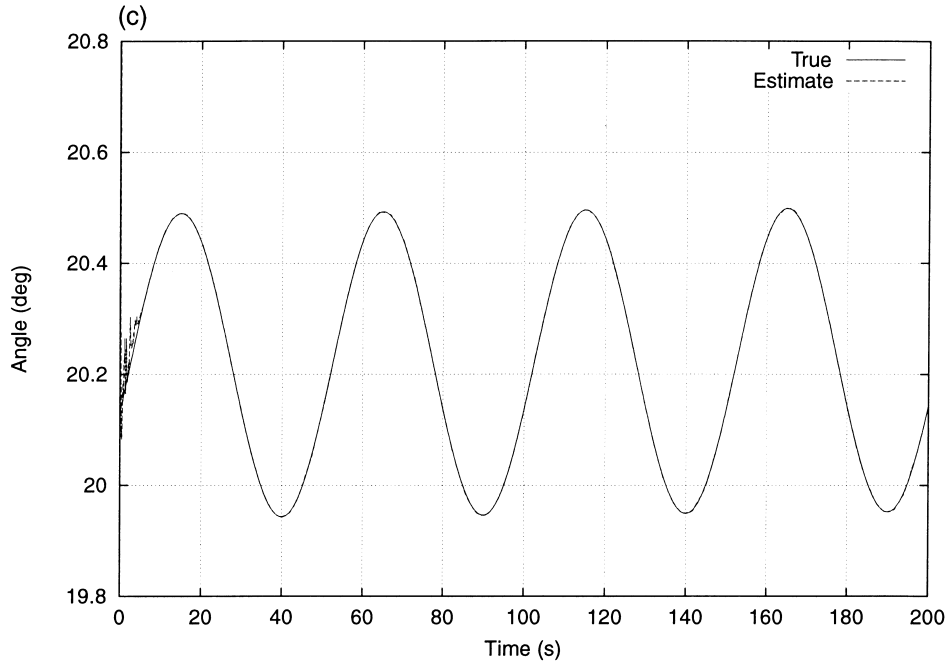


Fig. 2 (continued)

Being a special case of the orthogonal Procrustes problem, the matrix orthogonalization problem can be easily solved using the singular value decomposition (SVD). Thus, if

is the SVD of the matrix  $\hat{D}(k+1|k+1)$  where  $U(k+1)$  and  $V(k+1)$  are the left and right singular vector matrices, respectively, and  $\Sigma(k+1)$  is the singular value matrix, then

$$\hat{D}(k+1|k+1) = U(k+1)\Sigma(k+1)V^T(k+1) \quad \hat{D}^*(k+1|k+1) = U(k+1)V^T(k+1) \quad (57)$$

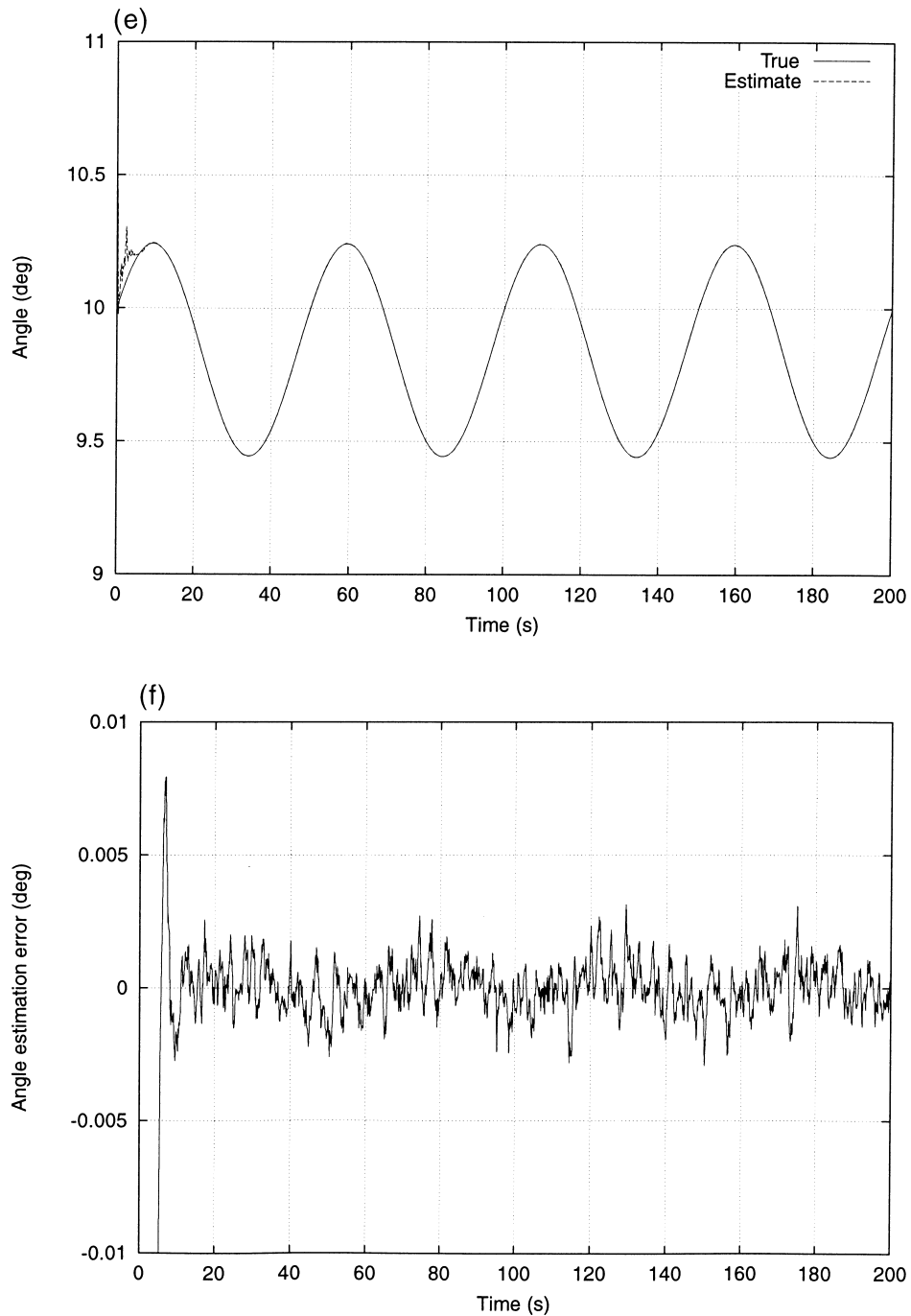


Fig. 2 (continued)

The excessive computational burden associated with the SVD might render its use prohibitive in certain applications, e.g., in *real-time* attitude control systems under computational power constraints. In such cases, an alternative, approximate orthogonalization scheme, which constitutes a single iteration of

the iterative orthogonalization algorithm introduced in Ref. [12], can be used. According to that scheme, an improved (nearly orthogonal), *a posteriori* estimate for the attitude matrix, is computed as

$$\hat{D}^*(k+1 | k+1) = N(k+1)\hat{D}(k+1 | k+1) \quad (58)$$

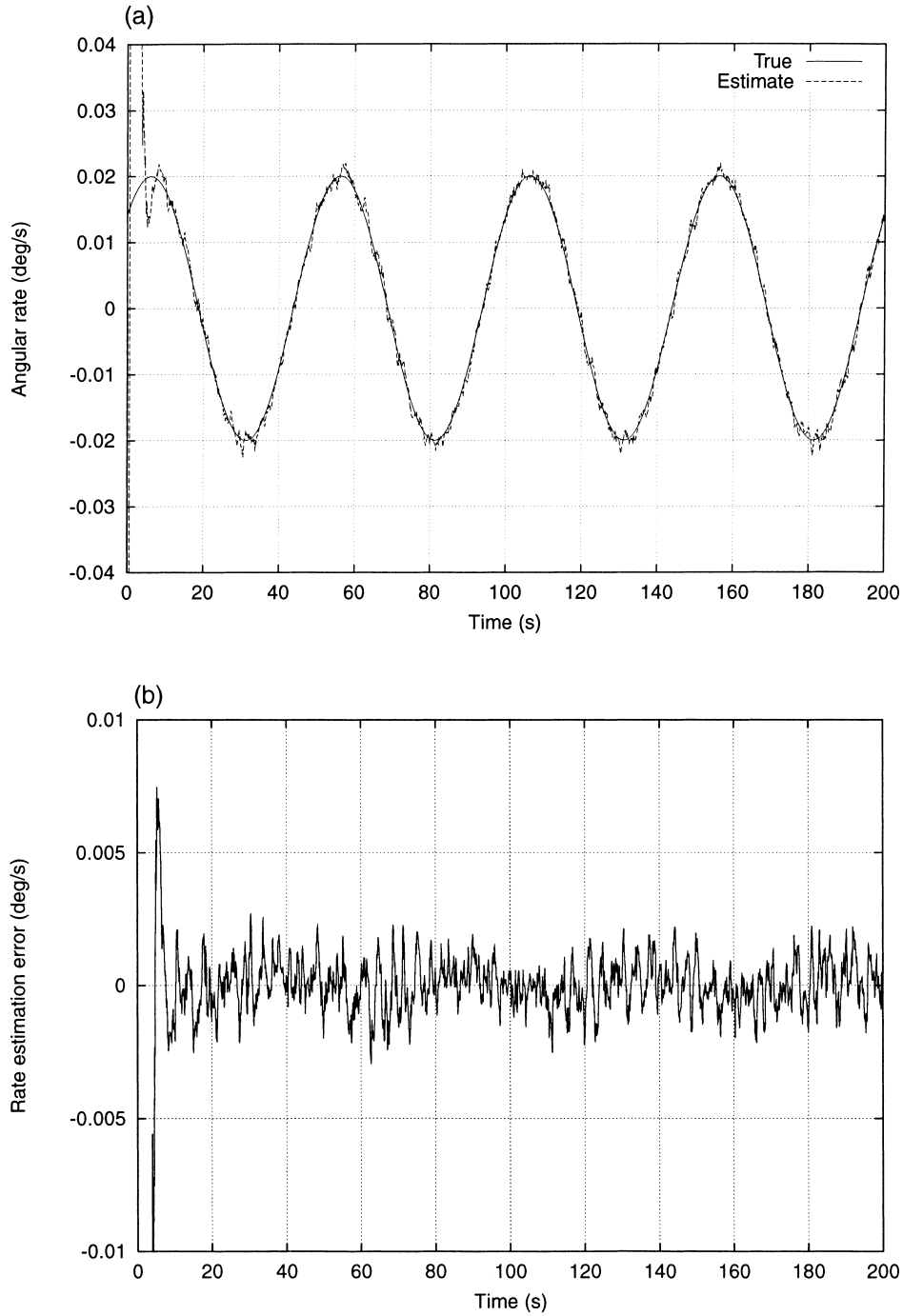


Fig. 3. Estimated vs true angular velocity components in a typical simulation run. (a)  $\omega_1$ . (b)  $\omega_1$  estimation error. (c)  $\omega_2$ . (d)  $\omega_2$  estimation error. (e)  $\omega_3$ . (f)  $\omega_3$  estimation error.

where the linear transformation that maps the *a posteriori* attitude matrix into its orthogonalized version is

$$N(k+1) \triangleq \frac{3}{2}I - \frac{1}{2}\hat{D}(k+1|k+1)\hat{D}^T(k+1|k+1)$$

As presented herein, the orthogonalization step is performed after each measurement update. However, in practice it was found that using the orthogonalization procedure also after the time propagation step, during the filter transient period, improves the filter's convergence rate.

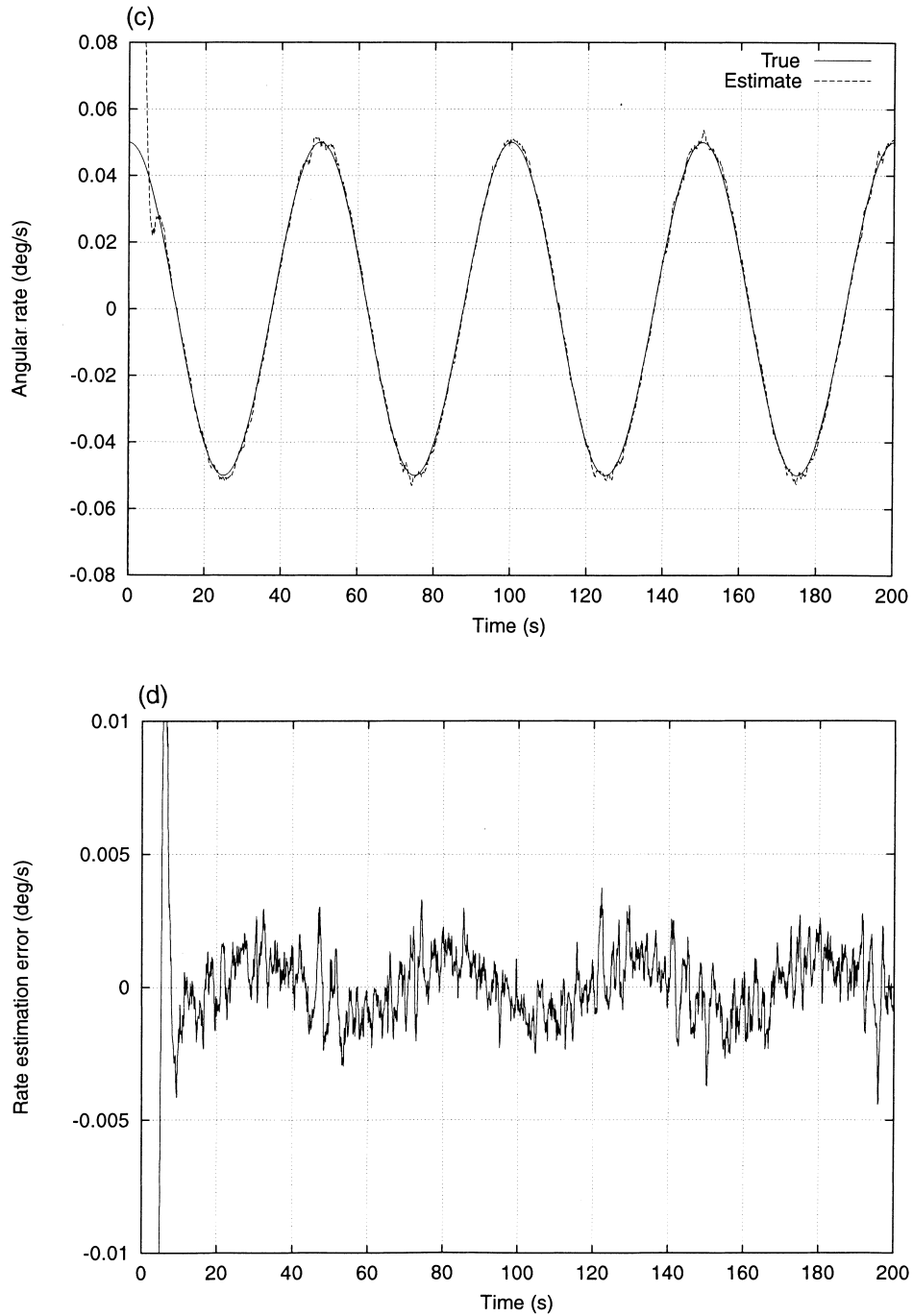


Fig. 3 (continued)

6. PREDICTION

In the prediction step at  $t_k$ , the reset *a posteriori* estimate at time  $t_k$ ,  $\hat{x}_f^c(k|k)$  [computed with the reset IRP estimate according to eqn (55)] and its corresponding error covariance matrix,  $P(k|k)$ , are propagated to time  $t_{k+1}$ .

Using eqn (26), we have

$$\hat{x}_f(k+1|k) = \Phi(T)\hat{x}_f^c(k|k) \quad (59)$$

Using this result with eqn (26) yields the covariance propagation equation

$$P(k+1|k) = \Phi(T)P(k|k)\Phi^T(T) + \Gamma(T)Q_f(k)\Gamma^T(T) \quad (60)$$

To propagate the attitude matrix to  $t_{k+1}$  we use the most recent IRP and attitude-rate estimates,  $\hat{\theta}(k+1|k)$  and  $\hat{\omega}(k|k)$ , respectively, and the ortho-

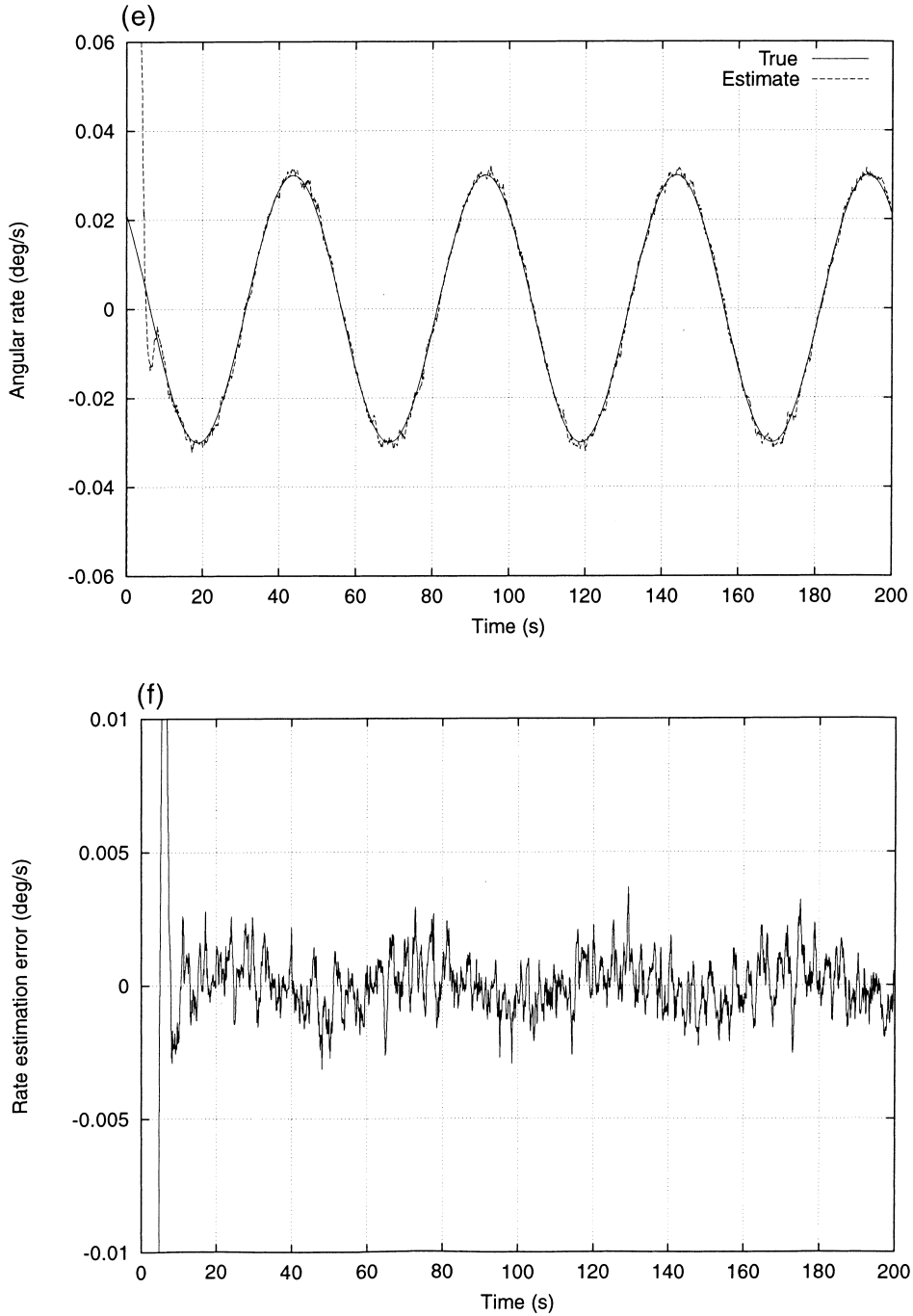


Fig. 3 (continued)

gonalized DCM estimate corresponding to  $t_k$ , in eqn (14). This yields

$$\begin{aligned} \hat{D}(k+1|k) = & \left\{ I + \bar{A}(k+1, k) + \frac{1}{2} \bar{A}^2(k+1, k) \right. \\ & + \frac{1}{6} \bar{A}^3(k+1, k) \\ & + \frac{1}{6} T \left[ \bar{A}(k+1, k) \hat{\Omega}(k|k) \right. \\ & \left. \left. - \hat{\Omega}(k|k) \bar{A}(k+1, k) \right] \right\} \hat{D}^*(k|k) \quad (61) \end{aligned}$$

where the *a priori* estimates of  $A(k+1, k)$  and  $\Omega(k)$  are defined as

$$\bar{A}(k+1, k) \triangleq - \left[ \hat{\theta}(k+1|k) \times \right] \quad (62)$$

$$\hat{\Omega}(k|k) \triangleq - \left[ \hat{\omega}(k|k) \times \right] \quad (63)$$

### 7. NUMERICAL STUDY

To demonstrate the performance of the new estimator, a numerical Monte Carlo simulation study was performed, in which simulated vector measurements were processed to obtain estimates of the attitude matrix and attitude rate. The estimated DCM was compared to the true attitude matrix using the following convergence and orthogonality metrics, respectively

$$\begin{aligned} J_c(k+1) & \triangleq \frac{1}{M} \sum_{n=1}^M \left\| \hat{D}_n^*(k+1|k+1) - D_n(k+1) \right\| \\ J_0(k+1) & \triangleq \frac{1}{M} \sum_{n=1}^M \left\| \hat{D}_n^{*T}(k+1|k+1) \right. \\ & \quad \left. \times \hat{D}_n^*(k+1|k+1) - I \right\| \end{aligned}$$

where  $M$  is the number of simulation runs. *Both* the body-frame and the reference frame vector measurements were contaminated by zero-mean, white, Gaussian noise sequences, orthogonal to the true directions, with  $R_v = \sigma_v^2 I$ ,  $R_u = \sigma_u^2 I$ , where the noise equivalent angles were  $\sigma_u = \sigma_v = 5$  arcsec. The initial attitude estimate was set to the identity matrix (thus assuming that  $\mathcal{S}_u$  and  $\mathcal{S}_v$  coincide at  $t_0$ ) while the true attitude corresponded to Euler angles of 30 deg, 20 deg and 10 deg in roll, pitch and yaw, respectively. The true angular velocity of  $\mathcal{S}_v$  relative to  $\mathcal{S}_u$  was

$$\omega(t) = \begin{bmatrix} 0.02 \\ 0.05 \\ 0.03 \end{bmatrix} \sin \left( \frac{2\pi}{50} t + \begin{bmatrix} \pi/4 \\ \pi/2 \\ 3\pi/4 \end{bmatrix} \right) \text{ deg/s} \quad (64)$$

while the initial angular velocity estimate was set to zero. The filter was run at a rate of 20 Hz, i.e., the sampling interval was  $T = 0.05$  s, while the measure-

ment processing rate was 10 Hz. The angular acceleration model parameters were:  $\tau = 10$  s,  $\dot{\omega}_M = 10^{-4}$  rad/s<sup>2</sup>,  $p_M = p_0 = 0.001$  for all three axes.

The performance indices obtained from a 100-run Monte Carlo simulation are presented in Fig. 1. In spite of its poor initial estimates, the estimator converged in all runs to an accurate and orthogonal DCM estimate after a relatively short transient period, thus demonstrating its robustness.

In Fig. 2, the three Euler angles, their estimates (computed using the estimated attitude matrix, assuming a 3-2-1 Euler angle sequence) and their corresponding estimation errors are shown for a typical run. The average Euler angle steady-state estimation error in a typical run was on the order of 0.1 arcsec, while the estimation error standard deviation was on the order of 3 arcsec.

In Fig. 3, the three components of the angular velocity vector, their estimates and their corresponding estimation errors are shown for a typical run. After the estimator's convergence period, the average rate estimation error was smaller than 0.04 arcsec/s, and the error standard deviation was on the order of 3.6 arcsec/s.

### 8. CONCLUSIONS

In this paper we have presented a computationally efficient, nonlinear estimator, that directly uses vector measurements to estimate both the attitude matrix and the angular velocity, avoiding the need to precompute the temporal derivatives of these noisy measurements. The algorithm is based on the recently introduced IRP third-order minimal parametrization of the attitude matrix, which is at the heart of its computational efficiency. Avoiding the use of the uncertain spacecraft dynamic model, the filter uses a polynomial state space model, in which the spacecraft angular acceleration is modeled as an exponential correlation stochastic process, a concept used in tracking theory.

Simulation results have been presented, that demonstrate the accuracy and robustness of the proposed algorithm.

*Acknowledgements*—This work was performed while the first author held a National Research Council — NASA Goddard Space Flight Center Research Associateship.

### REFERENCES

1. Lefferts, E. J., Markley, F. L. and Shuster, M. D., Kalman filtering for spacecraft attitude estimation. *Journal of Guidance, Control, and Dynamics*, 1982, **5**(5), 417–429.
2. Gai, E., Daly, K., Harrison, J. and Lemos, L., Star-sensor-based satellite attitude/attitude rate estimator. *Journal of Guidance, Control, and Dynamics*, 1985, **8**(5), 560–565.
3. Challa, M., Natanson, G. and Wheeler, C., Simultaneous determination of spacecraft attitude and

- rates using only a magnetometer. In *Proceedings of the AIAA/AAS Astrodynamics Specialist Conference*. AIAA, Washington, DC, 1996 San Diego, CA, July.
4. Azor, R., Bar-Itzhack, I. Y. and Harman, R. H., Satellite angular rate estimation from vector measurements. In *Proceedings of the AIAA Guidance, Navigation and Control Conference*. AIAA, Washington, DC, 1996 San Diego, CA, August.
  5. Crassidis, J. L. and Markley, F. L., Predictive filtering for attitude estimation without rate sensors. *Journal of Guidance, Control, and Dynamics*, 1997, **20**(3), 522–527.
  6. Ronen, M. and Oshman, Y., A third-order, minimal-parameter solution of the orthogonal matrix differential equation. *Journal of Guidance, Control, and Dynamics*, 1997, **20**(3), 516–521.
  7. Oshman, Y. and Markley, F. L., Minimal-parameter attitude matrix estimation from vector observations. In *Proceedings of the AIAA Guidance, Navigation and Control Conference*. AIAA, Washington, DC, 1997 New Orleans, LA, August.
  8. Bar-Shalom, Y. and Fortmann, T. E., *Tracking and Data Association*. Academic Press, San Diego, CA, 1988.
  9. Oshman, Y. and Bar-Itzhack, I. Y., Eigenfactor solution of the matrix Riccati equation — a continuous square root algorithm. *IEEE Transactions on Automatic Control*, 1985, **AC-30**(10), 971–978.
  10. Bar-Itzhack, I. Y. and Markley, F. L., Minimal parameter solution of the orthogonal matrix differential equation. *IEEE Transactions on Automatic Control*, 1990, **AC-35**(3), 314–317.
  11. Mendel, J. M., *Lessons in Digital Estimation Theory*. Prentice-Hall, New Jersey, 1987.
  12. Bar-Itzhack, I. Y. and Meyer, J., On the convergence of iterative orthogonalization processes. *IEEE Transactions on Aerospace and Electronic Systems*, 1976, **AES-12**, 146–151.